

Neural Network Verification through Replication

Mauro J. Sanchirico III, Dr. Xun Jiao, and Dr. C. Nataraj

Abstract—A system identification based approach to neural network model replication is presented and the application of model replication to verification of fundamental, single hidden layer, neural network systems is demonstrated. The presented approach serves as a means to partially address the problem of verifying that a neural network implementation meets a provided specification given only grey-box access to the implemented network. The procedure developed involves stimulating a neural network with a chosen signal, extracting a replicated model from the response, and systematically checking that the replicated model is output-equivalent to a specified model in order to verify that the grey-box system under test is implemented to specification without direct access to its hidden parameters. The replication step is introduced to provide an inherent guarantee that the stimulus signals employed yield sufficient test coverage. This method is investigated as a neural network focused nonlinear counterpart to the traditional verification of circuits through system identification. A strategy for choosing the stimulus is provided and an algorithm for verifying that the resulting response is indicative of a specification-compliant neural network system under test is derived. We find that the method can reliably detect defects in small neural networks or in small sub-circuits within larger neural networks.

Index Terms—Neural Networks, Replication, Verification, System Identification.

I. INTRODUCTION

IN the design and test of control and signal processing systems, methods whereby a system under test is stimulated with a signal so that system performance parameters can be inferred from the resulting response are of fundamental importance. For a linear system under test, such methods comprise the cannon of linear system identification and provide a basis for the comparison of control system performance [1]. For nonlinear systems, choice of the stimulus signal and parameter identification strategy often incur system specific challenges to be addressed [2]. In this paper, we present a system identification based strategy for determining the weights of fundamental neural network systems and subsystems, and apply the technique to verify that a small neural network or small component of a larger neural network meets a given specification.

Inspired by multi-sinusoidal system identification techniques developed for electrical and electro-mechanical systems [3] [4] [5] [6] [7] [8], the procedure involves stimulating a suitably small neural network or a fundamental sub-circuit inside a larger network with a sinusoid of a different frequency at each input simultaneously. Then, following the methods of model stealing / replication [9] [10] [11] [12] [13], a replicated neural network is fit to match the measured response

M. Sanchirico and X. Jiao are with the Department of Electrical and Computer Engineering, Villanova University, Villanova, PA, 19085 USA

C. Nataraj is with the Department of Mechanical Engineering, Villanova University, Villanova, PA, 19085 USA

Network Unit Test Procedure

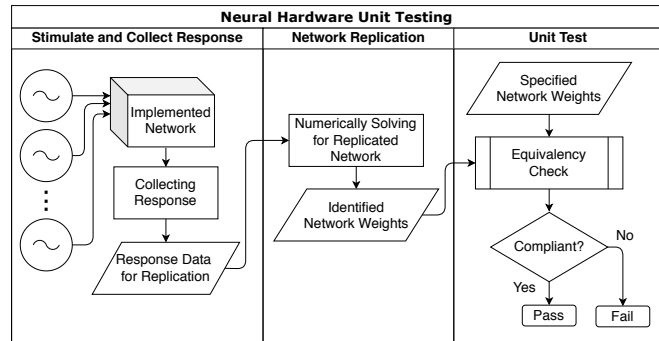


Fig. 1. Unit level test procedure applying network replication to verify implemented neural network hardware or sub-circuits / sub-networks within a neural network. An implemented network of known structure with unknown weights is stimulated by sinusoids of different frequencies and the unknown weights are identified from the response. The identified weights are checked for equivalency to the specified weights to determine if the implemented network is compliant.

for the given stimulus. Because the weights of a replicated network are not guaranteed to match the original due to the existence of symmetric configurations of the same weights [14] [15] or output-equivalent networks with different weights [16], we introduce a systematic method to check if the weights of the replicated network represent a network with behavior equivalent to the specification. The equivalency check accepts the weights of two networks as inputs, and returns a measure of similarity indicating if the two neural networks will have approximately equivalent output under certain assumptions. The full test process employing the replication step is summarized in Figure 1.

The model replication step is used to provide the test engineer with a guarantee that the stimulus applied yields suitable coverage to achieve a comprehensive test. If the signal does not provide sufficient test coverage, the model replication step will fail and the test will fail as a result. A failed test is therefore indicative of (a) an insufficient test signal or (b) a network defect. Introduction of this step biases the test towards a low false negative rate of defect detection while offering the test engineer high confidence in a passing result and the opportunity to further inspect a failed result by switching to a more comprehensive test signal. We offer this procedure as a bridge between traditional system identification, network replication, and the task of verifying that a network has been implemented to meet a specification.

To frame an exemplary problem encountered by the artificial intelligence practitioner and addressed by this work, we offer for consideration a neural network that is to be used in the controls or signal processing chain of a fielded hardware system. Examples of fielded systems which may have neural controls

include unmanned aerial vehicles [17] [18] and hypersonic vehicles [19]. Examples of neural network applications in signal processing chains include signal amplification [20], microphone adaptation in automatic speech recognition systems [21], and matched filtering [22] [23] [24]. We desire to verify neural network sub-components or sub-circuits in these types of systems using test signals similar to those that could be used to test a nonlinear circuit.

In such applications, it is often advantageous for practitioners to design a neural network in software and then implement it in hardware, taking full advantage of both the rapid development capabilities offered by open-source software tools [25] [26] [27] and the run-time efficiency offered by numerous proposed neural network hardware implementation approaches [28] [29] [30] [31]. However, separating design from implementation in this manner carries a need to answer the question: how might a test procedure be designed to enable a test engineer to verify that the neural network implemented in hardware meets the specification provided by the original designer?

The need for neural network verification has been recognized for decades [32] and early work emphasizes the need for system requirements and software testing [33] [34]. An early reference on neural network verification and validation is provided by Taylor [35]. In our work we apply the classical definitions for verification (*building the system right*) and validation (*building the right system*) from this text, and seek to verify that the network was *built right*. While verification of neural networks has since been researched in the context of defense against adversarial attack [36] [37] and output reachable set estimation [38], verification that a neural network meets a provided specification remains an open need [39]. Addressing the need is first complicated by the fact that multiple equivalent symmetric configurations of specified network weights exist [14] [15] and by the fact that small perturbations in parameters can yield approximately equivalent input-output relationships [16]. The problem is further complicated by the fact that the test engineer may not have access to the proprietary data-set used by the designer for training and testing.

One naive solution to these challenges would be for the test procedure to mandate disassembling the network hardware to check each weight individually. However, this would be impractical for large networks and might not be possible for networks implemented in embedded hardware. Furthermore, even if the test engineer could extract each weight individually, the weights implemented in hardware might not match the specification exactly due to inevitable imprecisions. Due to nonlinearity, changes in weights are not directly proportional to the resulting changes in output. Thus, it is unclear what degree of deviation represents a defect.

To address these challenges, we propose combining well-known system identification techniques for nonlinear circuits with recent neural network model replication techniques to verify that a neural network or sub-circuit within a neural network is implemented to specification in a manner analogous to the way a traditional circuit would be verified: apply a stimulus, measure the response, extract a model, check if the extracted model meets the specification. This approach

Use Case for a Network Unit Test

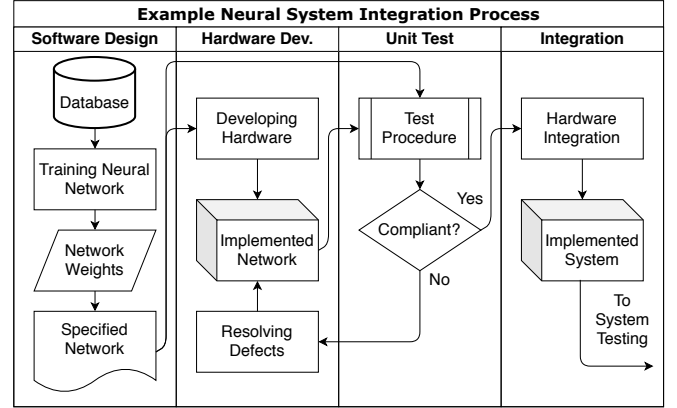


Fig. 2. Example use case of a test for network specification compliance showing how unit level compliance testing fits into a larger system development process before integration and system level testing. A software design firm trains a network on a proprietary data set and then provides a specification to a hardware manufacturing firm to implement the network. The software firm then provides the specification to a third party tester who must check that the implemented network is compliant with the specification before allowing a systems integrator to integrate the network with a larger system.

eliminates the need to test weights individually. Instead, small neural networks can be tested holistically as grey-boxes and large neural networks can be tested as collections of individual sub-circuits such as those identified in recent work [40] [41] [42] [43]. The full procedure therefore enables artificial intelligence practitioners to design a neural network in software, specify its weights and architecture for implementation in hardware, and provide both the hardware and specification to a third party to test for compliance. The ability to do so with grey-box access and without sharing a common data-set could enable effective cross-organizational collaboration and third party testing without sharing proprietary data-sets. An example system integration process that could make use of these methods is shown in Figure 2.

A. Definitions

We define the *specified network* to be the neural network, or a sub-circuit thereof, that was specified by the designer, such as a software engineer who executed the original learning process from a proprietary data-set that may not be provided to the test engineer. Similarly, we define the *network under test* to be the implemented neural network (e.g. in hardware), or a sub-circuit thereof, which a test engineer must verify meets the designer's specification. The *stimulus signal* is the signal applied by the test engineer and the *response signal* is the signal measured by the test engineer, including measurement noise.

The *replicated network* is defined to be the neural network having weights extracted from the network under test by the test engineer, or a sub-circuit thereof. A network under test is verified to be a *compliant network* if the replicated network is *output-equivalent* to the specified network and is called a *defective network* otherwise. Two networks are determined to be output-equivalent if it is shown that they will produce

sufficiently close outputs for all inputs in a given interval, according to a provided error metric. We define *verification* to mean the process by which a test engineer confirms that a network under test is compliant with the designer's provided specification.

B. Assumptions

To facilitate rigorous analysis of small fundamental neural network circuits, several simplifying assumptions were made. The relaxation of these assumptions will be a direction for future work.

- 1) *Multi-layered perceptron (MLP) architecture*: In order to clarify the exposition, a fundamental, single hidden layer, single output neural network (i.e. MLP) is chosen as the subject of this study. A hyperbolic tangent activation and fully connected layers are assumed.
- 2) *Bounded inputs*: We assume that the test engineer knows the largest possible magnitudes of all network inputs (e.g. the test engineer knows how the input was normalized). Without loss of generality, we use inputs x_i normalized such that $x_i \in [-1, 1]$.
- 3) *Bounded weights*: In order to provide a rigorous guarantee that a replicated network is output-equivalent to a specified network, we also assume that the test engineer knows the largest possible magnitude that a first layer network weight can have. This value can be provided by the design engineer in the specification. We note that an incorrectly provided weight bound will be immediately apparent to the test engineer because resultant calculations will clearly diverge.
- 4) *Low-dimensional inputs*: In order to allow visualizing the inputs of the network and the classification boundary, a two input network is used to generate figures. Formulas are provided for n-dimensional inputs. The issue of increasing computational complexity with input dimensionality is discussed and potential solutions are proposed.
- 5) *Grey-box access*: It is assumed that the engineer executing the model replication and verification procedures has grey-box access to the neural network under test. Grey-box access is taken to mean that the test engineer knows the expected architecture of the network under test, including the number of hidden neurons, but does not have direct access to the weights and their configuration.

C. Contributions

Our contributions are as follows:

- A system identification based approach to neural network model replication is presented, including a strategy for choosing stimulus signals and a means of deducing expected characteristics of the resulting response signals.
- An equivalency test procedure for checking that a replicated network is output-equivalent to a specified network is derived and offered as a means of verifying that a network under test is compliant with a specification. The equivalency test operates directly on the weights of two

networks, computing its similarity metric directly from the weights identified for the network under test and the specified weights.

- A means of expanding a hyperbolic tangent activated neural network as a multivariate polynomial is provided as a fundamental enabling technique for system identification based model replication and equivalency checking, and for analysis of neural network sub-circuits.

The rest of this paper is organized into an overview of the method, a derivation of an enabling polynomial expansion for the approach, an exposition of the model replication and verification technique, a summary of experimental results, and a discussion of related work, extensions, and limitations.

II. PROPOSED METHOD OVERVIEW

Consider a multi-layer perceptron neural network having number of inputs N_I and number of hidden neurons N_H . The network's input layer weights and biases are denoted $W^{\{0\}} = [w_{n,i}^{\{0\}}] \in \mathcal{M}^{N_H \times N_I}$ and $b^{\{0\}} = [b_n] \in \mathcal{M}^{N_H \times 1}$. Its hidden layer weights and bias are denoted $w^{\{1\}} = [w_n^{\{1\}}] \in \mathcal{M}^{1 \times N_H}$ and $b^{\{1\}} \in \mathcal{M}^{1 \times 1}$. The network has the activation function $\varphi(v) = \tanh(v)$. The weights and biases for a given network are collectively denoted β .

$$\beta = \{W^{\{0\}}, w^{\{1\}}, b^{\{0\}}, b^{\{1\}}\} \quad (1)$$

Such a network has the input-output relationship:

$$y(\beta, x) = w^{\{1\}} \tanh(W^{\{0\}}x + b^{\{0\}}) + b^{\{1\}} \quad (2)$$

The input to hidden neuron n is denoted v_n :

$$v_n = b_n^{\{0\}} + \sum_{i=1}^{N_I} w_{n,i}^{\{0\}} x_i \quad \forall n \in [1, N_H] \quad (3)$$

The proposed method begins with a hardware network under test having implemented weights and biases β_I . The test engineer needs to verify that implemented weights β_I are compliant with specified network weights β_S . This might take place during the unit test step in the example neural network system integration process shown in Figure 2.

A. Stimulus and Response

The test engineer activates an interrogation signal x_I to set each input of the implemented neural network to a sinusoid of a different frequency:

$$x_I = \begin{pmatrix} \sin(\omega_1 t) \\ \sin(\omega_2 t) \\ \vdots \\ \sin(\omega_{N_I} t) \end{pmatrix} \quad (4)$$

The measured output of the implemented network with any incurred measurement noise \mathcal{N} is collected and denoted:

$$y_M = y(\beta_I, x_I) + \mathcal{N} \quad (5)$$

B. Network Replication

The input and measurement output pairs (x_I, y_M) are then used to numerically solve for the replicated network weights β_R by solving:

$$\beta_R = \arg \min_{\beta} \left((y_M - y(\beta, x_I))^2 \right) \quad (6)$$

The minimization is subject to the constraint that each element of β_R has a magnitude less than the maximum weight in the specification, i.e. $\beta_i < \max(\beta_S) \quad \forall \beta_i \in \beta_R$. This constraint must be applied because the expansion used to test the equivalency of the replicated neural network with the specified neural network is valid only for a given range of hidden neuron inputs.

C. Equivalency Check

To assess if β_R produces a neural network output-equivalent to β_S we apply a polynomial expansion to the hyperbolic tangent activation function.

$$\tanh(v) \simeq \sum_{m=1}^M \alpha_{2m-1} v^{2m-1} \quad (7)$$

The expansion is derived in the following section and enables the specified and replicated neural networks to be represented as multivariate polynomials having coefficients $\Psi(\beta_S) = (\Psi_1(\beta_S) \quad \Psi_2(\beta_S) \quad \cdots \quad \Psi_N(\beta_S))$ and $\Psi(\beta_R) = (\Psi_1(\beta_R) \quad \Psi_2(\beta_R) \quad \cdots \quad \Psi_N(\beta_R))$ respectively. To check equivalency, we use an inverse hyperbolic sine scaled mean difference between the coefficients:

$$E(\Psi(\beta_R), \Psi(\beta_S)) = \text{mean} \left(\left| \operatorname{asinh} \left(\frac{\Psi(\beta_S)}{2} \right) - \operatorname{asinh} \left(\frac{\Psi(\beta_R)}{2} \right) \right| \right) \quad (8)$$

The error metric of equation 8 was judiciously chosen to account for the large variability in the size of the coefficients. Larger numerical errors are less significant for large coefficients than they would be for smaller coefficients. If all coefficients were positive, a standard logarithmic error metric could be employed to compress the error signals. Since the coefficients are signed, we instead apply inverse hyperbolic sine scaling to achieve similar compression without yielding undefined errors for negative coefficients.

If $E(\Psi(\beta_R), \Psi(\beta_S)) < \varepsilon$, where ε is a specified tolerance, then the network under test is declared compliant. Otherwise, the network under test is declared defective. Figure 1 shows the stimulus/response, replication, and verification (unit test) steps. The polynomial expansion, stimulus/response signals, and verification methods are elaborated on in the following sections.

III. A MODIFIED POLYNOMIAL EXPANSION

To facilitate understanding of the expected characteristics of a network under test's response to a given stimulus, and to facilitate the expansion to be used in the equivalency test, we require a polynomial expansion in the form of equation

7. The Taylor series of equation 9 is of a suitable form but converges only for arguments $|v| < \frac{\pi}{2}$ and therefore hinders practical analysis of networks where activation function inputs take larger values, i.e. $W_I^{\{0\}} x + b_I^{\{0\}} \geq \frac{\pi}{2}$.

$$\tanh(v) \simeq \sum_{m=1}^M \frac{2^{2m} (2^{2m} - 1) B_{2m}}{(2m)!} v^{2m-1}, \quad |v| < \frac{\pi}{2} \quad (9)$$

To address this need, we introduce an expansion which can be made valid on a chosen interval $(-v_{MAX}, v_{MAX})$ by using coefficients $\alpha_j(M)$ adjusted to account for the number of terms M in the expansion. The expansion is developed by applying Fourier inversion to express the hyperbolic tangent in terms of its own Fourier sine transform:

$$\tanh(v) = \lim_{\rho \rightarrow \infty} \int_0^{\rho} \operatorname{csch} \left(\frac{\pi}{2} \xi \right) \sin(\xi v) d\xi \quad (10)$$

To achieve a polynomial expansion, the kernel $\sin(\xi v)$ is expanded to a partial sum via Taylor series. To avoid integrating into the divergent region of the expansion, the upper bound of the integral is replaced with an upper bound $\rho_v(M)$ adjusted for (1) the number of terms M used in the expansion and (2) the maximum anticipated value of v , v_{MAX} .

$$\tanh(v) \simeq \sum_{m=1}^M \int_0^{\rho_v(M)} \xi^{2m-1} \operatorname{csch} \left(\frac{\pi}{2} \xi \right) d\xi \frac{(-1)^{m-1} v^{2m-1}}{(2m-1)!} \quad (11)$$

We define the range of validity of the M term partial sum of $\sin(u)$ to be equal to $\rho(M)$ where $\rho(M)$ is the largest real part of its complex roots.

$$\rho(M) = \max(\Re \{r_M\}) \quad (12)$$

In equation 12, r_M is the collection of complex roots of the M term partial sum of $\sin(u)$:

$$r_M = u \in \mathbb{C} \quad \text{s.t.} \quad \sum_{m=1}^M \frac{(-1)^{m-1} u^{2m-1}}{(2m-1)!} = 0 \quad (13)$$

Since the argument to the sinusoid in equation 11 is $u = \xi v$, the integration bounds can be adjusted for the maximum argument of the hyperbolic tangent, v_{MAX} , by noting that $u = \rho(M)$ implies $\xi = \frac{\rho(M)}{v}$. To err on the side of conservatism, we adjust ρ by the maximum of v .

$$\rho_v(M) = \frac{\rho(M)}{v_{MAX}} \quad (14)$$

An expansion of the hyperbolic tangent valid on the desired interval $(-v_{MAX}, v_{MAX})$ can then be defined by rearranging equation 11 and solving the integral.

$$\tanh(v) \simeq \sum_{m=1}^M \alpha_j(M) v^j, \quad j = 2m - 1 \quad (15)$$

$$\alpha_j(M) = \frac{(-1)^{m-1}}{j!} \left(\Lambda_j(\rho_v(M)) - \lim_{\epsilon \rightarrow 0} \Lambda_j(\epsilon) \right) \quad (16)$$

Algorithm for Generating the $\Psi_\kappa(\beta)$ Coefficients

$$\Lambda_j(\xi) = \int \xi^j \operatorname{csch}(a\xi) d\xi = \sum_{k=1}^{j+1} \frac{j! \xi^{j-k+1}}{a^k (j-k+1)!} (\operatorname{Li}_k(-e^{a\xi}) - \operatorname{Li}_k(e^{a\xi})) \quad (17)$$

In equation 17 the parameter a is set to $\frac{\pi}{2}$. The range of validity $\rho(M)$ in equation 12 and the anti-derivatives of equation 17 can be precomputed and saved along with the α coefficients of equation 15. We call the expansion of equations 15 – 17 a modified expansion of the hyperbolic tangent. These coefficients can then be used to expand the network under test as a multivariate polynomial. To perform this expansion, we substitute the hidden neuron input as defined in equation 3 into equation 15.

$$\tanh(v_n) \simeq \sum_{m=1}^M \alpha_j \left(b_n^{\{0\}} + \sum_{i=1}^{N_I} w_{n,i}^{\{0\}} x_i \right)^j, \quad j = 2m - 1 \quad (18)$$

Applying multinomial expansion:

$$\tanh(v_n) \simeq \sum_{m=1}^M \sum_{|\kappa|=j} \alpha_j \binom{j}{\kappa} \vartheta_n^\kappa x^\kappa \quad (19)$$

$$\vartheta_n = \left(b_n^{\{0\}} \quad w_{n,1}^{\{0\}} \quad \dots \quad w_{n,N_I}^{\{0\}} \right) \quad (20)$$

Here $\kappa = (\kappa_1, \kappa_2, \dots, \kappa_{N_I+1})$ is a multi-index where $w^\kappa = \prod_i u_i^{\kappa_i}$, $|\kappa| = \sum_i \kappa_i$, and $\binom{j}{\kappa} = \frac{j!}{\kappa_1! \kappa_2! \dots \kappa_N!}$ is a multinomial coefficient. The output of the network can then be approximated by taking the output weighted sum of the neuron outputs:

$$y(\beta, x) \simeq b^{\{1\}} + \sum_{n=1}^{N_H} \sum_{m=1}^M \sum_{|\kappa|=j} \alpha_j(M) \binom{j}{\kappa} w_n^{\{1\}} \vartheta_n^\kappa x^\kappa \quad (21)$$

We use $\Psi_\kappa(\beta)$ to denote the coefficient associated with the term $x^\kappa = x^{\kappa_1} x^{\kappa_2} \dots x^{\kappa_{N_I+1}}$ in the polynomial approximation of $y(\beta, x)$. By definition of $\Psi_\kappa(\beta)$ we can write:

$$y(\beta, x) \simeq \sum_{\kappa} \Psi_\kappa(\beta) x^\kappa \quad (22)$$

We use $\Psi(\beta)$ to denote the collection of all $\Psi_\kappa(\beta)$ coefficients. The algorithm of Figure 3 can be used to generate $\Psi(\beta)$ given the activation function expansion constants α and the collection of weights β .

IV. NETWORK REPLICATION AND VERIFICATION DETAILS

The network replication procedure begins with the application of a stimulus signal vector of the form of equation 4 to the inputs of the network under test having implemented weights β_I . Sinusoidal stimulus signals are used to ensure the response signal is periodic and thus easy to measure in its entirety. Since the response signal as given in equation 21 is

```

Input:  $\alpha, \beta$ 
Output:  $\Psi$ 
1: Initialize new map  $\Psi : \text{tuple} \rightarrow \text{double}$ 
2: for  $n = 1 \dots N_H$  do
3:    $\vartheta_n \leftarrow \left( b_n^{\{0\}} \quad w_{n,1}^{\{0\}} \quad \dots \quad w_{n,N_I}^{\{0\}} \right)$ 
4:   for  $m = 1 \dots M$  do
5:      $j \leftarrow 2m - 1$ 
6:      $\mathcal{K} \leftarrow$  all multi-indices  $\kappa$  s.t.  $\sum_{i=1}^{N_I+1} \kappa_i = j$ 
7:     for  $\kappa \in \mathcal{K}$  do
8:       if ( $\Psi_\kappa$  is set) then
9:          $\Psi_\kappa \leftarrow \Psi_\kappa + \alpha_j(M) \binom{j}{\kappa} w_n^{\{1\}} \vartheta_n^\kappa$ 
10:      else
11:         $\Psi_\kappa \leftarrow \alpha_j(M) \binom{j}{\kappa} w_n^{\{1\}} \vartheta_n^\kappa$ 
12:      end if
13:    end for
14:  end for
15: end for
16: return  $\Psi$ 

```

Fig. 3. Algorithm for generating $\Psi_\kappa(\beta)$ coefficients. The inputs of the algorithm are the activation function expansion constants α and the collection of network weights and biases β . The output is a hashmap data structure mapping multi-indices κ (represented as tuples) to their corresponding $\Psi_\kappa(\beta)$ coefficient. For each power in the expansion of the activation of each hidden neuron, the corresponding set of multi-indices are generated to expand the sum in equation 21. If the Ψ coefficient for the current multi-index has already been generated the result of the computation for the current multi-index is added to the existing value such that the resulting map can be used to evaluate the sum of equation 22.

a weighted sum of the multiples of the components of the stimulus signal vector, it can be inferred that the fundamental period of the response signal can be computed as the least common multiple of the periods of the individual stimulus signals. Measuring the response for the duration of at least one fundamental period guarantees the full capture of the response signal.

Of the individual frequencies selected for the components of the test signal vector, we desire a combination that provides (1) good coverage of the network's output surface and (2) yields a response signal with a short fundamental period thus resulting in a quick but comprehensive capture of the network under test's output surface. We use Shannon entropy as a measure of the coverage provided by a stimulus signal. We compute the Shannon entropy of a given stimulus signal by considering the signal sampled in discrete time well above the Nyquist rate, and then treating each combination of discrete values as a symbol ς_i . As such, the entropy H of the stimulus signal x is given $H(x) = -\sum_i P(\varsigma_i) \log P(\varsigma_i)$. As is well known in the analysis of nonlinear circuits [3], stimulus signals with components having frequencies that are integer multiples of other components do not provide sufficient coverage to serve as test signals.

An example signal that provides good entropy without

yielding a large fundamental period is:

$$x = \begin{pmatrix} \sin(5t) \\ \sin(4t) \end{pmatrix} \quad (23)$$

An example signal that provides better entropy at the cost of a larger fundamental period is:

$$x = \begin{pmatrix} \sin(11t) \\ \sin(10t) \end{pmatrix} \quad (24)$$

Our observations of the reliability of the verification procedure are shown with respect to stimulus signal choice in Figure 8.

Once the response to the stimulus signal is measured, we need to solve for the weights β_R of a replicated network having empirically output-equivalent performance to the implemented network, since we do not have direct access to the weights β_I of the implemented network. This is achieved through numerically solving equation 6 subject to the constraints listed in section II-B. We apply a trust region reflective algorithm, however other constrained nonlinear optimization techniques could be substituted to identify β_R .

With the weights β_R of the replicated network identified, we need to determine if the replicated network is output-equivalent to the specified network β_S in order to make the final assessment about whether the network under test is compliant with the specification. To make this assessment without yielding false failures due to equivalent configurations of the same network or innocuous perturbations of the weights, we compare the Ψ coefficients of each network $\Psi(\beta_S)$ and $\Psi(\beta_R)$ instead of comparing the weights directly. We compute these coefficients according to the algorithm of Figure 3. Applying the error metric of equation 8, we determine if the error between $\Psi(\beta_S)$ and $\Psi(\beta_R)$ is greater than an acceptable tolerance ε . Based on our observations in tuning ε shown in Figure 12, we choose $\varepsilon = 1$ as our tolerance to use in the collection of experimental results.

V. EXPERIMENTAL RESULTS

A. Experimental Setup

To collect experimental results, we begin by demonstrating the accuracy of the modified expansion method employed to derive the equivalency test, and then move on to assess the validity of the equivalency test using a set of illustrative experimental configurations. We then computationally model the process of stimulating the network under test, collecting the responses with measurement noise (modeled as white Gaussian), identifying a replicated network, and checking the replicated network for compliance. We determine the optimal error threshold ε by varying ε for a population of 150 defective and 150 compliant networks and recording the true and false positive rates of defect detection (Figure 1) with respect to ε . We then instantiate a group of 100 networks and introduce defects into 50 of them. We run the procedure of Figure 1 on each network and track how many of the defects were identified. We repeat the process with increasing amounts of measurement noise and observe effects on defect identification statistics.

Hyperbolic Tangent Approximation

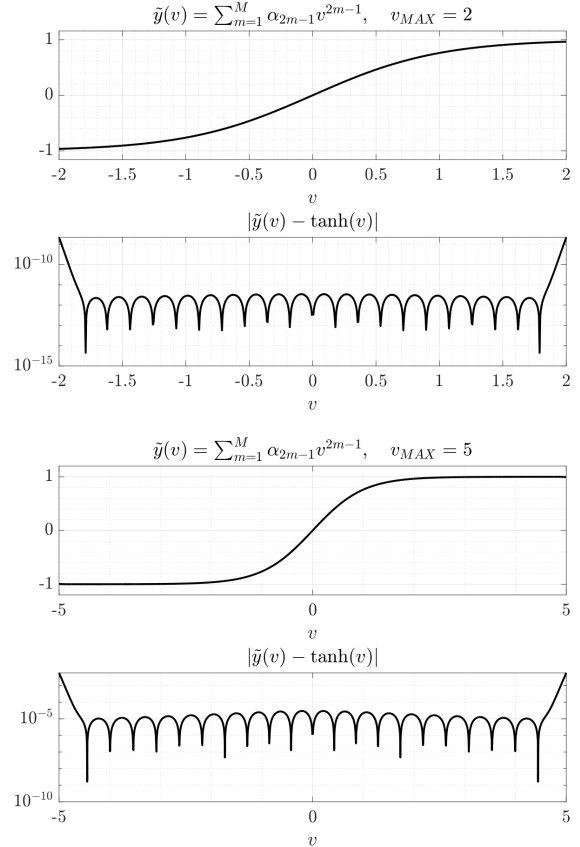


Fig. 4. The results of a modified expansion of the hyperbolic tangent are shown. The modified expansion provides a v_{MAX} parameter which can be increased to extend its region of convergence outside the region of convergence of the straightforward Taylor series. The plots above show the results of the expansion for $v_{MAX} = 2$ and $v_{MAX} = 5$, along with the error between each expansion and the true hyperbolic tangent. Sums were evaluated using $M = 40$.

B. Hyperbolic Tangent Expansion Technique

The methods of this paper are enabled by a modified polynomial expansion of the hyperbolic tangent, defined in equations 15–17, which we apply to achieve a polynomial expansion of a small neural network or sub-circuit within a neural network. The modified expansion provides a user-adjustable region of convergence which can be made to extend outside the region of convergence of the Taylor series. Here we present results showing the accuracy of the expansion itself within its region of convergence. The region of convergence can be extended by increasing the v_{MAX} parameter. In Figure 4, we show plots of the evaluated expansion $\tilde{y}(v) = \sum_{m=1}^M \alpha_{2m-1} v^{2m-1}$ and the error $|\tilde{y}(v) - \tanh(v)|$ between the expansion and the true hyperbolic tangent for $v_{MAX} = 2$ and $v_{MAX} = 5$. In both cases, $M = 40$ is used to evaluate the sum. In Figure 5, the error between the expansion and the true hyperbolic tangent is shown, for $v_{MAX} = 2$ and $v_{MAX} = 5$, with respect to the argument of the hyperbolic tangent v and the number of terms applied in the expansion.

Hyperbolic Tangent Approximation Convergence

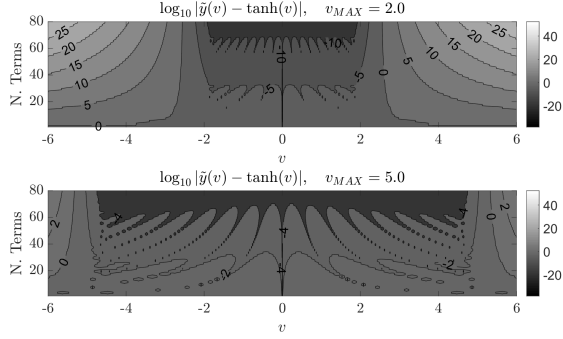


Fig. 5. The error between the modified expansion of the hyperbolic tangent and the true hyperbolic tangent is shown with respect to the argument v and the number of terms used in the expansion. Even powered terms which are always zero in the expansion of the hyperbolic tangent are counted in the number of terms, so 80 terms equates to $M = 40$. The expansion with $v_{MAX} = 5$ has a wider region of convergence but requires more terms to reach an error as small as the expansion having $v_{MAX} = 2$. Both expansions diverge rapidly outside their region of convergence.

Stimulus and Response Signals

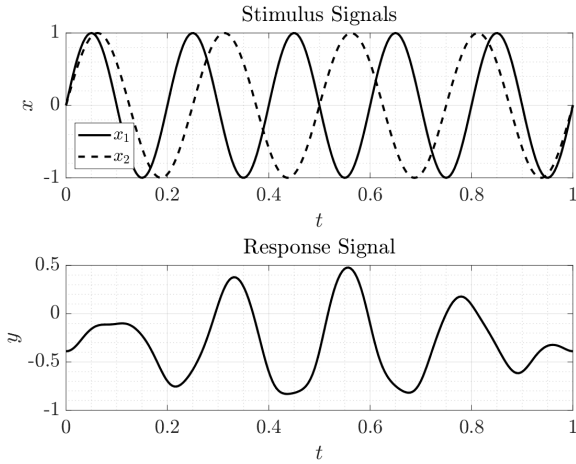


Fig. 6. An example stimulus signal and its resulting response signal are shown. The stimulus signal has two components: $x_1(t) = \sin(5t)$ and $x_2(t) = \sin(4t)$. The resulting response shown is the output of a random network under test under application of this stimulus signal.

C. Stimulus and Response Signals

The example stimulus signal x of equation 23 is shown in Figure 6 along with the resulting response $y(\beta, x)$ for a randomly selected small network under test with two inputs, three hidden neurons, and a single output. The same stimulus signal's coverage of the circuit's output contours is shown in Figure 7. The output of same small neural circuit is shown with respect to its input components x_1 and x_2 . The path that the stimulus signal takes across the output contours is shown.

To assess the effect of stimulus choice on the accuracy of the verification procedure, we execute the verification procedure of Figure 1 over a population of 100 networks, where 50 have randomly introduced defects. Each network represents a small neural circuit having two inputs, three hidden neurons, and one output. We repeat the verification procedure using stimulus

Stimulus Signal and Network Output Contours

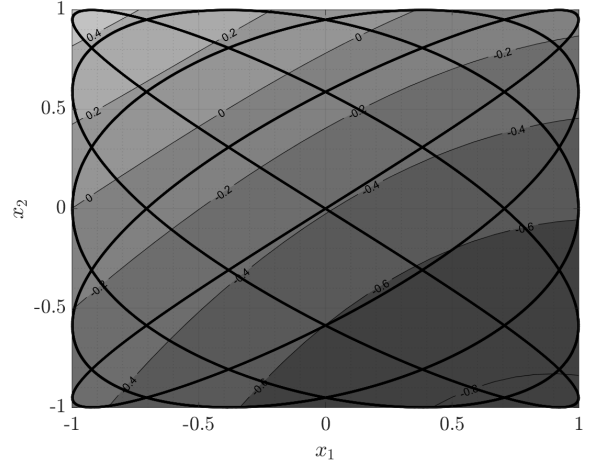


Fig. 7. The path that an example stimulus signal follows over the contours of a random network under test is shown as a black line. The output of the network over any (x_1, x_2) pair is shown as a contoured surface. The stimulus signal has two components: $x_1(t) = \sin(5t)$ and $x_2(t) = \sin(4t)$.

Effect of Stimulus Signal Choice on Accuracy of Defect Detection Procedure

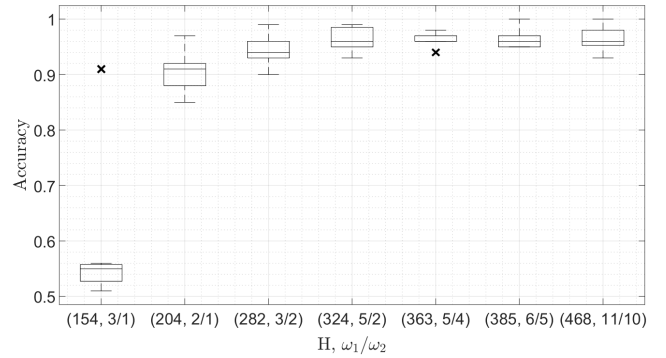


Fig. 8. Defect detection accuracy is shown for several stimulus signals. Accuracy statistics were computed over a population of 50 defective networks and 50 compliant networks. The verification procedure was run on each network with a measurement SNR of 100 dB, and the experiment was repeated using several stimulus signals 10 rounds each using different random noise each round. Stimulus signal entropy H is shown along with the frequency ratio of the stimulus signal components $\frac{\omega_1}{\omega_2}$. We observe that non-integer ratios between ω_1 and ω_2 provide higher entropy and a more reliable test.

signals having several (ω_1, ω_2) pairs and observe how many of the defects are correctly identified to compute the accuracy of the procedure for each stimulus signal. The entire experiment was repeated 10 times using different random measurement noise and introducing new random defects each round. In this experiment, defects are created by introducing random changes to the weights of the network under test. We observe that non-integer ratios between selected stimulus signal frequencies provide higher signal entropy and that higher entropy stimulus signals result in more reliable detection of the defective networks.

D. Testing the Equivalency Test

To determine if checking the error between the Ψ coefficients using the error metric of equation 8 is a valid means to assess the equivalency of different sets of specified and replicated network weights, we conduct four experiments, where different kinds of equivalent and non-equivalent networks are compared:

- 1) In an *exactly equivalent networks* experiment we instantiate two copies of the same network and demonstrate that the error metric $E(\Psi(\beta_1), \Psi(\beta_2))$ of equation 8 is zero for $\beta_1 = \beta_2$.
- 2) In a *symmetrically equivalent networks* experiment we instantiate two networks with weights rearranged in obviously symmetric configurations such as those discussed by Sussmann [14] and Albertini [15]. We demonstrate that the error metric E is still zero for these symmetric configurations.
- 3) In a *approximately equivalent networks* experiment we instantiate two copies of the same network and introduce in one network a small perturbation in the hidden layer weights (i.e. after the nonlinear activation) to cause a proportionally small change in the input-output relationship. We demonstrate that in this case E is non-zero but still small, as is desired behavior.
- 4) In a *nonequivalent networks* experiment we instantiate two completely different networks and demonstrate that E is large, as is desired behavior.

In each experiment, a two input, three hidden neuron, single output circuit with random weights is used as a test case. The circuit is duplicated and the duplicate modified in a manner that will result in either an equivalent or non-equivalent circuit. We expect to observe a larger error metric for non-equivalent circuits than for equivalent circuits. We observe $E = 0$ in the exactly equivalent networks test. The results of the symmetrically equivalent networks test, the approximately equivalent networks test, and the non-equivalent networks test are shown in Figures 9, 10, 11 respectively. In the symmetrically equivalent networks test, we observe $E = 0$. In the approximately equivalent networks test, we observe $0 < E < 1$. In the non-equivalent networks test, we observe $E > 1$.

E. Verifying a Population of Networks Under Test

To confirm that $E < \varepsilon$, $\varepsilon = 1$ is a valid condition for determining equivalent networks, we perform a test where the error threshold is swept and the accuracy of the procedure of Figure 1 is recorded with respect to the threshold. A population of 300 small neural circuits is instantiated, each having two inputs, three hidden neurons, and one output. These networks under test could represent a small standalone non-linear circuit or small components of a larger neural network being analyzed. We select 150 of the 300 small networks under test and introduce defects into them by adding random perturbations to the existing weights. The correct weights are saved off as the specified network weights. We run the defect detection procedure using different error tolerances spanning from $\varepsilon = 10^{-6}$ to $\varepsilon = 10^2$ and track the true positive and false

Symmetrically Equivalent Networks Comparison

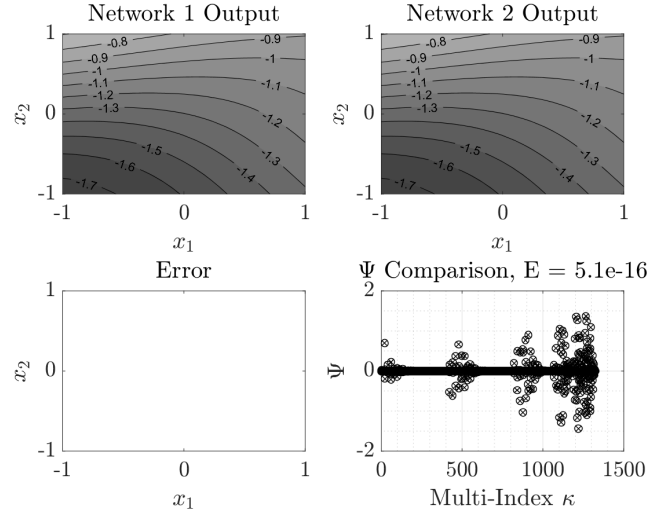


Fig. 9. Output contours over a 2D input space are shown for two symmetrically equivalent neural networks. The symmetrically equivalent networks were generated by creating two exactly equivalent networks and exchanging neurons in one of the networks to create a network with the same behavior as the first but with a different configuration of the same weights. The $\Psi_\kappa(\beta_1)$ and $\Psi_\kappa(\beta_2)$ coefficients match exactly as is expected behavior.

Approximately Equivalent Networks Comparison

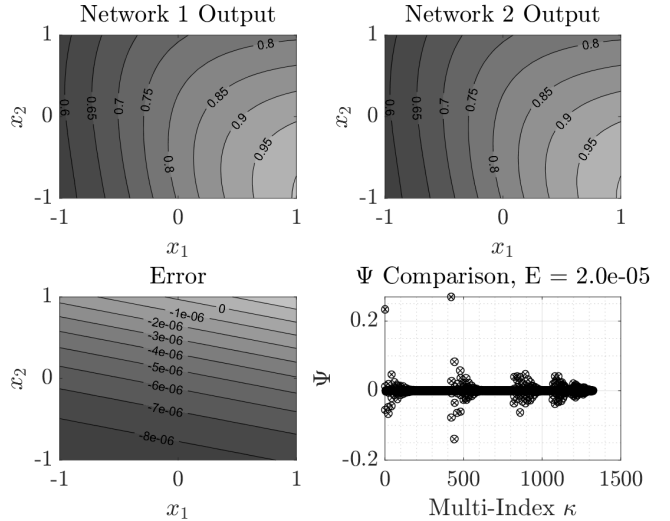


Fig. 10. Output contours over a 2D input space are shown for two approximately equivalent neural networks. The approximately equivalent networks were generated by creating two exactly equivalent networks and introducing into one of the networks a small error that does not noticeably affect performance and thus does not represent a defect. The $\Psi_\kappa(\beta_1)$ and $\Psi_\kappa(\beta_2)$ coefficients match closely as is expected, yielding an error metric $E(\Psi(\beta_1), \Psi(\beta_2)) < 1.0$.

positive rates of the test, where a true positive is a correctly identified defect and a false positive is an incorrectly identified defect. The error tolerance sweep is repeated with signal to measurement noise ratios of 25dB, 50dB, and 100dB.

We find that $\varepsilon = 1$ provides a suitable balance between low false positive rates and high true positive rates. False and true positive rates are shown in Figure 12. We observe that false

Non-Equivalent Networks Comparison

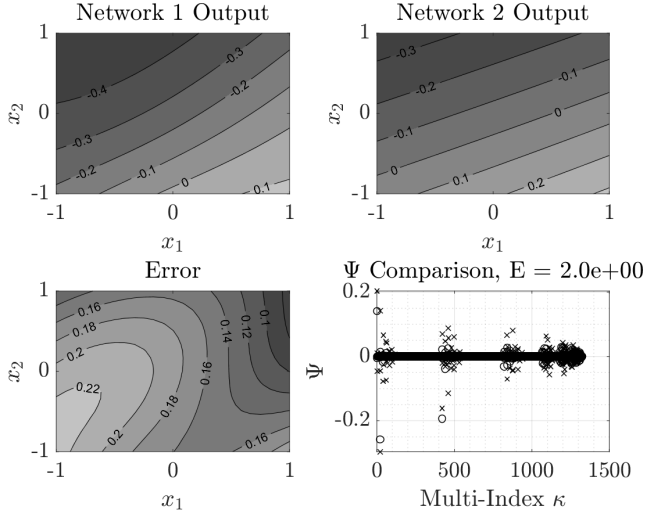


Fig. 11. Output contours over a 2D input space are shown for two non-equivalent neural networks. The two non-equivalent networks were generated by randomly perturbing the weights of two exactly equivalent networks. The $\Psi_{\kappa}(\beta_1)$ and $\Psi_{\kappa}(\beta_2)$ coefficients do not match and yield an error metric $E(\Psi(\beta_1), \Psi(\beta_2)) > 1.0$ as is expected.

Defect Detection True and False Positive Rates with Respect to Error Tolerance ε

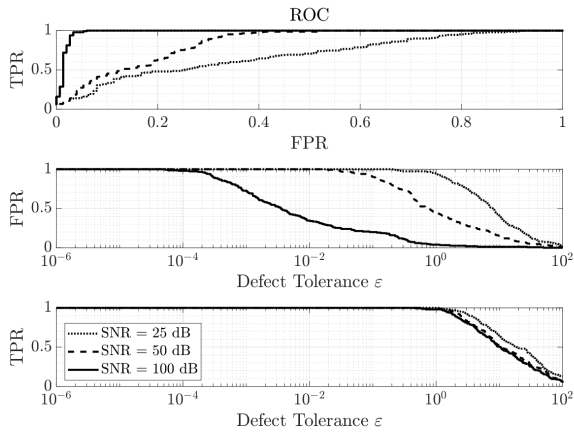


Fig. 12. Receiver Operating Characteristic curves are shown for the verification procedure. A population of 150 defective networks and 150 compliant networks were used to generate the curves. The $\Psi_{\kappa}(\beta)$ coefficients were computed for all networks and the verification procedure was executed with different defect tolerances ε . The entire experiment was repeated using different signal to noise ratios.

positives are caused by the optimizer failing to replicate the network under test in the time allowed (we limit the number of function evaluations to 10K, and limit the number initial seeds the solver is allowed to try to 20 to keep run times consistent). A false positive could be rectified by allowing the optimizer to run longer on potentially defective networks under test.

With a suitable tolerance for identification of non-equivalent networks determined, we create a population of 100 networks, where 50 are compliant with the corresponding specified network and 50 have defects. We run the defect detection

Defect Detection Accuracy wrt. Signal to Noise Ratio

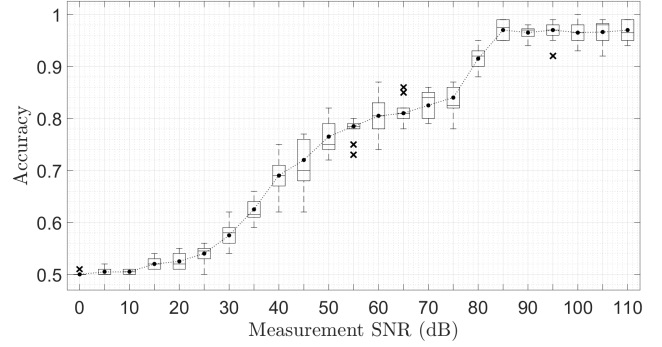


Fig. 13. Defect detection accuracy with respect to signal to measurement noise ratio is shown. Accuracy statistics were computed over a population of 50 defective networks and 50 compliant networks. The verification procedure was run on each network for each measurement SNR shown. The entire experiment was repeated 10 times for each SNR with different random measurement noise for a total of 23000 calls to the test procedure. Mean and median accuracy are shown as black dots and black lines respectively.

procedure of Figure 1 on all 100 networks for measurement signal to noise ratios between 0dB and 110dB and observe the accuracy of the defect identification procedure. We repeat the entire procedure 10 times with different random defects and different random noise. Observed test procedure accuracy with respect to measurement SNR is summarized in Figure 13.

VI. DISCUSSION AND RELATED WORK

This work is intended to connect traditional system identification with neural network replication and neural system or subsystem verification, and therefore builds off the methods of linear and nonlinear system identification. These methods are combined with neural network replication approaches to address challenges in neural network verification. As such, this work provides several paths to extensions and connects to several areas of neural network research including network replication attack and defense, network verification, equivalency, and neural sub-circuit level interpret-ability.

A. Relationship to Replication Attacks and Defenses

Neural network replication as a form of model stealing attack wherein a surrogate model is trained to have similar classification performance as a target model is well explored [9] [10] [11] [12] [13]. Here we build off the methods of neural network replication, re-purposing the *avatar model* [11] or *knockoff net* [13] approach for the white-hat application of neural system or subsystem verification. To meet the specific needs of the verification application, we have contributed a model replication approach which (1) reproduces the network's output surface for inputs in the bounded range and (2) yields test signal responses that take an expected form (distorted sinusoids with known fundamental period), even for a neural network with unknown weights.

As a direction for future work, we propose further experimentation with the use of various model replication strategies

as a form of verification, building off the fundamental concept that introducing a replication step into the verification procedure provides an inherent guarantee of test signal coverage, since test signals with insufficient coverage will cause the replication step to fail. Furthermore, defenses against replication attacks for neural systems deployed on neuromorphic hardware are presented by Yang et al. [44] and a software based defense against replication attacks for public prediction interfaces is presented by Juuti et al. [45]. We propose that with further work replication approaches for verification could be combined with these approaches and with principles from cyber-security to enable replication for the purposes of system verification for authorized users while blocking replication for unauthorized users.

B. Neural Network Verification Methodology

A recent review of the state of the art in neural network verification and validation by Borg et al. highlights the need for methods of defining a formal specification for a neural network and for specifying test cases [39]. We offer our approach as a means to partially address this need, complementary to existing approaches addressing other aspects of the verification problem. Examples of recent work on neural network verification focus on defense against and identification of adversarial perturbations [36] [37], output reachable set estimation [38], and computing upper bounds on error rates under adversarial attack [46]. Liu et al. survey algorithms for verifying deep neural networks and divide them into the categories of reachability analysis, optimization to falsify an assertion, and search to falsify an assertion [47]. Bunel et al. present a unifying framework for the formal verification of piecewise linear neural networks (e.g. ReLU based) [48].

Furthermore, fuzz testing has also been presented as a means to address neural network verification challenges, particularly for networks implemented in software. White-box fuzz testing approaches with test coverage maximization strategies are available and demonstrated in recent work [49] [50] [51] [52]. These test strategies assume access to code and could be applied during software test stages to complement the methods presented here. As an extension to this paper and to the body of neural network test literature, we propose experimentation into the effectiveness of different test methods when employed at various stages of the system integration process of Figure 2, both as standalone tests and in connection with other test methods. We also propose investigation into the minimum stimulus signals required to guarantee successful model replication for networks of varying sizes.

C. Equivalent Neural Networks

Methods of identifying equivalent neural networks given a matrix of neuron outputs are available [53] [54] [55] [56] and have recently been advanced by Kornblith et al. [57]. Methods to identify opportunities for compressing a neural network [58] [59] and for perturbing parameters to identify output-equivalent neural networks are also available [16]. We offer as a complement to these works a method of checking neural network equivalence (i.e. checking network under test

compliance) by operating on the specified network weights and the replicated network weights without accessing the output signals of individual neurons.

D. Neural Network Sub-circuits and Interpretability

It has been recognized for decades that biological systems contain recurring fundamental circuit elements [60] and facilitate robust, invariant representations of objects [61]. However, it has only recently been demonstrated that trained neural networks contain interpretable cells or sub-circuits comprising semantic functions and algorithms [40] [41] [42] [62] [43]. Building on feature visualization methods such as those from Erhan et al. [63], Simonyan et al. [64], and Mordvintsev et al. [65], a number of methods are now available to visualize individual sub-circuits inside neural networks [66] [67] [68] [69] [70]. We offer the analysis methods of this paper as especially applicable to the detailed study of such small sub-circuits within larger neural networks and as a link between the study of traditional nonlinear circuits and these neural sub-circuits. We propose that the methods of this paper could be extended to provide a means of comparing neural circuits with different activations by extending the methods of section III, and could also be used in future work as a means of proving that a neural circuit has embodied a particular known mathematical function.

E. Limitations

The test procedure developed in this paper is intended to be applied to small fundamental systems, and as such, mathematical rigor was prioritized over speed of test execution. The test procedure calls for expanding a replicated network into a multivariate polynomial of Ψ coefficients using a modified expansion of the activation function, and as such has some limitations. The first limitation is that the input signals to each neuron must fall within the expansion's region of convergence. As the number of input neurons increase the size of the input signals to the activation functions increase. This challenge would be impossible to overcome using an unmodified expansion of the hyperbolic tangent, since the region of convergence is limited. The modified expansion was thus introduced to provide a user adjustable region of convergence which mitigates this challenge but does not eliminate it entirely. We propose to investigate how accurate the expansion can be made for very large inputs in future work to enable the relaxation of this limitation.

The second key limitation of expanding the activation functions as polynomials is that the number of terms in the expansion of the entire network grows rapidly with the number of inputs and the number of terms used in the expansion. While we intend for the method to initially be used to analyze small neural circuits, we propose that the scalability of the method can be improved by (1) dividing large networks into smaller sub-circuits to be analyzed individually, (2) parallelization of the algorithms used, and (3) non-exhaustive computation of and checking of the Ψ coefficients. The extent to which these such methods can improve scalability remains a direction for experimentation and analysis.

VII. CONCLUSION

This paper presents a system identification based approach to the replication of fundamental single hidden layer neural networks. The replication approach is applied to the verification of small neural networks or small sub-circuits within larger neural networks. We demonstrate that it is possible to confirm that a small grey-box network under test meets a given specification in a manner analogous to the system identification methods traditionally applied to nonlinear circuits: i.e. by stimulating the network with a given signal, extracting a replicated model from the response, and checking if the replicated model conforms to the specification. The procedure is enabled by an algorithm for checking the equivalency of two networks employing a modified polynomial expansion of the hyperbolic tangent.

Of the modified expansion, we conclude that the expressions derived yield the coefficients of a polynomial expansion of the hyperbolic tangent with an adjustable region of convergence suitable for analyzing strongly nonlinear behavior. The region of convergence can be extended outside that of the Taylor series therefore enabling the analysis of large input signals. Furthermore, we conclude that the modified expansion of the hyperbolic tangent can be applied to algorithmically determine a set of Ψ coefficients for a network under test which can be used to compare the network to other networks (e.g. to a specified network). The Ψ coefficients depend only on a set of constants α derived from the activation function using the modified expansion, and the weights β of the network under test. An error metric is provided for determining if two sets of Ψ coefficients represent two equivalent neural networks.

Of the application of network replication to verification, we conclude that neural circuits can be analyzed in a manner analogous to nonlinear electrical circuits and that for small neural circuits, the ability to replicate a grey-box network and confirm the replica's equivalence to a specification represents a reliable means of checking whether or not the network under test conforms to the specification. We conclude that the introduction of a replication step into the verification procedure provides an inherent check for test coverage as intended and note that this result is reflected in the fact that low coverage test signals yield a test with high recall / low precision, while high coverage test signals yield a sensitive and precise test.

Our planned directions for future work include: (1) investigation into the scalability of this method through both division of large networks into sub-circuits and algorithmic improvements such as parallelization and non-exhaustive checking of the Ψ coefficients; and (2) extension of the Ψ coefficients to other types of nonlinear activations to determine if Ψ coefficients can be used as a feature space inside of which non-homogeneous networks can be compared.

REFERENCES

- [1] K. Ogata, *Modern Control Engineering*. One Lake Street, Upper Saddle River, New Jersey 07458: Pearson, 2016.
- [2] L. A. Aguirre, "A Bird's Eye View of Nonlinear System Identification," *arXiv:1907.06803 [cs, eess]*, Jul. 2019, arXiv: 1907.06803. [Online]. Available: <http://arxiv.org/abs/1907.06803>
- [3] P. Wambacq and W. Sansen, *Distortion Analysis of Analog Integrated Circuits*, ser. The Kluwer International Series in Engineering and Computer Science, M. Ismail, Ed. Boston, MA: Springer US, 1998, vol. 451. [Online]. Available: <http://link.springer.com/10.1007/978-1-4757-5003-4>
- [4] A. Novk, L. Simon, F. Kadlec, and P. Lotton, "Nonlinear System Identification Using Exponential Swept-Sine Signal," *IEEE Transactions on Instrumentation and Measurement*, vol. 59, no. 8, pp. 2220–2229, Aug. 2010. [Online]. Available: <http://ieeexplore.ieee.org/document/5299278/>
- [5] M. T. Myslinski, D. M. M.-P. Schreurs, K. A. Remley, M. D. Mckinley, and B. Nauwelaers, "Large-signal behavioral model of a packaged rf amplifier based on qpsk-like multisine measurements," *European Gallium Arsenide and Other Semiconductor Application Symposium, GAAS 2005*, pp. 185–188, 2005.
- [6] D. Schreurs and K. A. Remley, "Use of multisine signals for efficient behavioural modelling of rf circuits with short-memory effects," in *61st ARFTG Conference Digest, Spring 2003.*, June 2003, pp. 65–72.
- [7] D. Schreurs, M. Myslinski, and C. A. Remley, "RF Behavioural Modelling from Multisine Measurements: Influence of Excitation Type," in *33rd European Microwave Conference 2003*, Munich, Germany, 2003.
- [8] M. Witters and J. Swevers, "Black-box identification of a continuously variable semi-active damper," in *2008 IEEE International Conference on Control Applications*, 2008, pp. 19–24.
- [9] F. Tramèr, F. Zhang, A. Juels, M. K. Reiter, and T. Ristenpart, "Stealing machine learning models via prediction apis," in *Proceedings of the 25th USENIX Conference on Security Symposium*, ser. SEC16. USA: USENIX Association, 2016, p. 601618.
- [10] N. Papernot, P. McDaniel, I. Goodfellow, S. Jha, Z. B. Celik, and A. Swami, "Practical Black-Box Attacks against Machine Learning," in *Proceedings of the 2017 ACM on Asia Conference on Computer and Communications Security - ASIA CCS '17*. Abu Dhabi, United Arab Emirates: ACM Press, 2017, pp. 506–519. [Online]. Available: <http://dl.acm.org/citation.cfm?doi=3052973.3053009>
- [11] S. J. Oh, B. Schiele, and M. Fritz, *Towards Reverse-Engineering Black-Box Neural Networks*. Cham: Springer International Publishing, 2019, pp. 121–144. [Online]. Available: https://doi.org/10.1007/978-3-030-28954-6_7
- [12] V. Duddu, D. Samanta, D. V. Rao, and V. E. Balas, "Stealing neural networks via timing side channels," *ArXiv*, vol. abs/1812.11720, 2018.
- [13] T. Orekondy, B. Schiele, and M. Fritz, "Knockoff Nets: Stealing Functionality of Black-Box Models," in *2019 IEEE/CVF Conference on Computer Vision and Pattern Recognition (CVPR)*. Long Beach, CA, USA: IEEE, Jun. 2019, pp. 4949–4958. [Online]. Available: <https://ieeexplore.ieee.org/document/8953839/>
- [14] H. J. Sussmann, "Uniqueness of the weights for minimal feedforward nets with a given input-output map," *Neural Networks*, vol. 5, no. 4, pp. 589–593, Jul. 1992. [Online]. Available: <https://linkinghub.elsevier.com/retrieve/pii/S0893608005800371>
- [15] F. Albertini and E. D. Sontag, "Uniqueness of Weights for Neural Networks," in *Artificial Neural Networks for Speech and Vision*. Chapman and Hall, London, 1993, pp. 113–125.
- [16] C. DiMattina and K. Zhang, "How to Modify a Neural Network Gradually Without Changing Its Input-Output Functionality," *Neural Computation*, vol. 22, no. 1, pp. 1–47, Jan. 2010. [Online]. Available: <http://www.mitpressjournals.org/doi/10.1162/neco.2009.05-08-781>
- [17] G. Lai, Z. Liu, Y. Zhang, and C. L. P. Chen, "Adaptive Position/Attitude Tracking Control of Aerial Robot With Unknown Inertial Matrix Based on a New Robust Neural Identifier," *IEEE Transactions on Neural Networks and Learning Systems*, vol. 27, no. 1, pp. 18–31, Jan. 2016. [Online]. Available: <http://ieeexplore.ieee.org/document/7061535/>
- [18] D. Nodland, H. Zargarzadeh, and S. Jagannathan, "Neural Network-Based Optimal Adaptive Output Feedback Control of a Helicopter UAV," *IEEE Transactions on Neural Networks and Learning Systems*, vol. 24, no. 7, pp. 1061–1073, Jul. 2013. [Online]. Available: <http://ieeexplore.ieee.org/document/6487408/>
- [19] B. Xu, D. Wang, Y. Zhang, and Z. Shi, "DOB-Based Neural Control of Flexible Hypersonic Flight Vehicle Considering Wind Effects," *IEEE Transactions on Industrial Electronics*, vol. 64, no. 11, pp. 8676–8685, Nov. 2017.
- [20] Xiaoming Liang, Liang Zhao, and Zonghua Liu, "Enhancing Weak Signal Transmission Through a Feedforward Network," *IEEE Transactions on Neural Networks and Learning Systems*, vol. 23, no. 9, pp. 1506–1512, Sep. 2012. [Online]. Available: <http://ieeexplore.ieee.org/document/6227359/>
- [21] S. M. Siniscalchi and V. M. Salerno, "Adaptation to New Microphones Using Artificial Neural Networks With Trainable Activation Functions,"

- IEEE Transactions on Neural Networks and Learning Systems*, vol. 28, no. 8, pp. 1959–1965, Aug. 2017. [Online]. Available: <http://ieeexplore.ieee.org/document/7452664/>
- [22] Q. Xue, Y. Hu, and W. Tompkins, “Neural-network-based adaptive matched filtering for QRS detection,” *IEEE Transactions on Biomedical Engineering*, vol. 39, no. 4, pp. 317–329, Apr. 1992. [Online]. Available: <http://ieeexplore.ieee.org/document/126604/>
- [23] H. Gabbard, M. Williams, F. Hayes, and C. Messenger, “Matching Matched Filtering with Deep Networks for Gravitational-Wave Astronomy,” *Physical Review Letters*, vol. 120, no. 14, p. 141103, Apr. 2018. [Online]. Available: <https://link.aps.org/doi/10.1103/PhysRevLett.120.141103>
- [24] D. George and E. Huerta, “Deep Learning for real-time gravitational wave detection and parameter estimation: Results with Advanced LIGO data,” *Physics Letters B*, vol. 778, pp. 64–70, Mar. 2018. [Online]. Available: <https://linkinghub.elsevier.com/retrieve/pii/S0370269317310390>
- [25] “scikit-learn: machine learning in Python scikit-learn 0.22.2 documentation.” [Online]. Available: <https://scikit-learn.org/stable/>
- [26] “PyTorch.” [Online]. Available: <https://www.pytorch.org>
- [27] “TensorFlow.” [Online]. Available: <https://www.tensorflow.org/>
- [28] J. Misra and I. Saha, “Artificial neural networks in hardware: A survey of two decades of progress,” *Neurocomputing*, vol. 74, no. 1-3, pp. 239–255, Dec. 2010. [Online]. Available: <https://linkinghub.elsevier.com/retrieve/pii/S092523121000216X>
- [29] D. Maliuk and Y. Makris, “An Experimentation Platform for On-Chip Integration of Analog Neural Networks: A Pathway to Trusted and Robust Analog/RF ICs,” *IEEE Transactions on Neural Networks and Learning Systems*, vol. 26, no. 8, pp. 1721–1734, Aug. 2015. [Online]. Available: <http://ieeexplore.ieee.org/lpdocs/epic03/wrapper.htm?arnumber=6901256>
- [30] A. M. Abdelsalam, J. M. P. Langlois, and F. Cheriet, “Accurate and Efficient Hyperbolic Tangent Activation Function on FPGA using the DCT Interpolation Filter,” *arXiv:1609.07750 [cs]*, Sep. 2016, arXiv: 1609.07750. [Online]. Available: <http://arxiv.org/abs/1609.07750>
- [31] C. D. Schuman, T. E. Potok, R. M. Patton, J. D. Birdwell, M. E. Dean, G. S. Rose, and J. S. Plank, “A Survey of Neuromorphic Computing and Neural Networks in Hardware,” *arXiv:1705.06963 [cs]*, May 2017, arXiv: 1705.06963. [Online]. Available: <http://arxiv.org/abs/1705.06963>
- [32] G. E. Peterson, “Foundation for neural network verification and validation,” in *Science of Artificial Neural Networks II*, D. W. Ruck, Ed., vol. 1966, International Society for Optics and Photonics. SPIE, 1993, pp. 196 – 207. [Online]. Available: <https://doi.org/10.1117/12.152651>
- [33] J. Schumann, P. Gupta, and S. Nelson, “On Verification and Validation of Neural Network Based Controllers,” NASA, Tech. Rep., 2003.
- [34] P. Gupta and J. Schumann, “A tool for verification and validation of neural network based adaptive controllers for high assurance systems,” in *Eighth IEEE International Symposium on High Assurance Systems Engineering, 2004. Proceedings*. Tampa, FL, USA: IEEE, 2004, pp. 277–278. [Online]. Available: <http://ieeexplore.ieee.org/document/1281757/>
- [35] B. J. Taylor, Ed., *Methods and procedures for the verification and validation of artificial neural networks*. New York, NY: Springer Science+Business Media, 2006.
- [36] B. Darvish Rouani, M. Samragh, T. Javidi, and F. Koushanfar, “Safe Machine Learning and Defeating Adversarial Attacks,” *IEEE Security & Privacy*, vol. 17, no. 2, pp. 31–38, Mar. 2019. [Online]. Available: <https://ieeexplore.ieee.org/document/8677311/>
- [37] A. Venzke and S. Chatzivasileiadis, “Verification of Neural Network Behaviour: Formal Guarantees for Power System Applications,” *arXiv:1910.01624 [cs, eess, math]*, Jan. 2020, arXiv: 1910.01624. [Online]. Available: <http://arxiv.org/abs/1910.01624>
- [38] W. Xiang, H.-D. Tran, and T. T. Johnson, “Output Reachable Set Estimation and Verification for Multilayer Neural Networks,” *IEEE Transactions on Neural Networks and Learning Systems*, vol. 29, no. 11, pp. 5777–5783, Nov. 2018. [Online]. Available: <https://ieeexplore.ieee.org/document/8318388/>
- [39] M. Borg, C. Englund, K. Wnuk, B. Duran, C. Levandowski, S. Gao, Y. Tan, H. Kaijser, H. Lnn, and J. Trnqvist, “Safely Entering the Deep: A Review of Verification and Validation for Machine Learning and a Challenge Elicitation in the Automotive Industry,” *Journal of Automotive Software Engineering*, vol. 1, no. 1, p. 1, 2019. [Online]. Available: <https://www.atlantis-press.com/article/125905766>
- [40] A. Karpathy, J. Johnson, and L. Fei-Fei, “Visualizing and Understanding Recurrent Networks,” *arXiv:1506.02078 [cs]*, Nov. 2015, arXiv: 1506.02078. [Online]. Available: <http://arxiv.org/abs/1506.02078>
- [41] B. Zhou, A. Khosla, A. Lapedriza, A. Oliva, and A. Torralba, “Object Detectors Emerge in Deep Scene CNNs,” *arXiv:1412.6856* [cs], Apr. 2015, arXiv: 1412.6856. [Online]. Available: <http://arxiv.org/abs/1412.6856>
- [42] D. Bau, B. Zhou, A. Khosla, A. Oliva, and A. Torralba, “Network Dissection: Quantifying Interpretability of Deep Visual Representations,” *arXiv:1704.05796 [cs]*, Apr. 2017, arXiv: 1704.05796. [Online]. Available: <http://arxiv.org/abs/1704.05796>
- [43] C. Olah, N. Cammarata, L. Schubert, G. Goh, M. Petrov, and S. Carter, “Zoom in: An introduction to circuits,” *Distill*, 2020, <https://distill.pub/2020/circuits/zoom-in>.
- [44] C. Yang, B. Liu, H. Li, Y. Chen, M. Barnell, Q. Wu, W. Wen, and J. Rajendran, “Thwarting Replication Attack against Memristor-based Neuromorphic Computing System,” *IEEE Transactions on Computer-Aided Design of Integrated Circuits and Systems*, pp. 1–1, 2019. [Online]. Available: <https://ieeexplore.ieee.org/document/8815820/>
- [45] M. Juuti, S. Szyller, S. Marchal, and N. Asokan, “PRADA: Protecting Against DNN Model Stealing Attacks,” in *2019 IEEE European Symposium on Security and Privacy (EuroS&P)*. Stockholm, Sweden: IEEE, Jun. 2019, pp. 512–527. [Online]. Available: <https://ieeexplore.ieee.org/document/8806737/>
- [46] K. Dvijotham, R. Stanforth, S. Gowal, C. Qin, S. De, and P. Kohli, “Efficient neural network verification with exactness characterization,” in *UAI*, 2019.
- [47] C. Liu, T. Arnon, C. Lazarus, C. W. Barrett, and M. J. Kochenderfer, “Algorithms for verifying deep neural networks,” *ArXiv*, vol. abs/1903.06758, 2019.
- [48] R. R. Buel, I. Turkaslan, P. Torr, P. Kohli, and P. K. Mudigonda, “A unified view of piecewise linear neural network verification,” in *Advances in Neural Information Processing Systems 31*, S. Bengio, H. Wallach, H. Larochelle, K. Grauman, N. Cesa-Bianchi, and R. Garnett, Eds. Curran Associates, Inc., 2018, pp. 4790–4799. [Online]. Available: <http://papers.nips.cc/paper/7728-a-unified-view-of-piecewise-linear-neural-network-verification.pdf>
- [49] K. Pei, Y. Cao, J. Yang, and S. Jana, “DeepXplore: Automated Whitebox Testing of Deep Learning Systems,” in *Proceedings of the 26th Symposium on Operating Systems Principles - SOSP '17*. Shanghai, China: ACM Press, 2017, pp. 1–18. [Online]. Available: <http://dl.acm.org/citation.cfm?doid=3132747.3132785>
- [50] J. Guo, Y. Jiang, Y. Zhao, Q. Chen, and J. Sun, “DLFuzz: differential fuzzing testing of deep learning systems,” in *Proceedings of the 2018 26th ACM Joint Meeting on European Software Engineering Conference and Symposium on the Foundations of Software Engineering - ESEC/FSE 2018*. Lake Buena Vista, FL, USA: ACM Press, 2018, pp. 739–743. [Online]. Available: <http://dl.acm.org/citation.cfm?doid=3236024.3264835>
- [51] A. Odena, C. Olsson, D. G. Andersen, and I. Goodfellow, “TensorFuzz: Debugging Neural Networks with Coverage-Guided Fuzzing,” in *Proceedings of the 36th International Conference on Machine Learning*, Long Beach, CA, USA, 2019, 2019.
- [52] J. Liang, Y. Jiang, M. Wang, X. Jiao, Y. Chen, H. Song, and K.-K. R. Choo, “DeepFuzzer: Accelerated Deep Greybox Fuzzing,” *IEEE Transactions on Dependable and Secure Computing*, pp. 1–1, 2019. [Online]. Available: <https://ieeexplore.ieee.org/document/8937483/>
- [53] A. Laakso and G. Cottrell, “Content and cluster analysis: Assessing representational similarity in neural systems,” *Philosophical Psychology*, vol. 13, no. 1, pp. 47–76, Mar. 2000. [Online]. Available: <http://www.tandfonline.com/doi/abs/10.1080/09515080050002726>
- [54] Y. Li, J. Yosinski, J. Clune, H. Lipson, and J. Hopcroft, “Convergent Learning: Do different neural networks learn the same representations?” in *Journal of Machine Learning Research Conference Proceedings*, 2015, pp. 196–212.
- [55] M. Raghu, J. Gilmer, J. Yosinski, and J. Sohl-Dickstein, “Svcca: Singular vector canonical correlation analysis for deep learning dynamics and interpretability,” in *Advances in Neural Information Processing Systems 30*, I. Guyon, U. V. Luxburg, S. Bengio, H. Wallach, R. Fergus, S. Vishwanathan, and R. Garnett, Eds. Curran Associates, Inc., 2017, pp. 6076–6085. [Online]. Available: <http://papers.nips.cc/paper/7188-svcca-singular-vector-canonical-correlation-analysis-for-deep-learning-dynamics-and-interpretability.pdf>
- [56] A. Morcos, M. Raghu, and S. Bengio, “Insights on representational similarity in neural networks with canonical correlation,” in *Advances in Neural Information Processing Systems 31*, S. Bengio, H. Wallach, H. Larochelle, K. Grauman, N. Cesa-Bianchi, and R. Garnett, Eds. Curran Associates, Inc., 2018, pp. 5727–5736. [Online]. Available: <http://papers.nips.cc/paper/7815-insights-on-representational-similarity-in-neural-networks-with-canonical-correlation.pdf>
- [57] S. Kornblith, M. Norouzi, H. Lee, and G. Hinton, “Similarity of Neural Network Representations Revisited,” in *Proceedings of the 36th*

International Conference on Machine Learning, Long Beach, CA, USA, 2019.

- [58] C.-H. Chang, “Deep and Shallow Architecture of Multilayer Neural Networks,” *IEEE Transactions on Neural Networks and Learning Systems*, vol. 26, no. 10, pp. 2477–2486, Oct. 2015. [Online]. Available: <http://ieeexplore.ieee.org/document/7010967/>
- [59] H. Huang and H. Yu, “LTNN: A Layerwise Tensorized Compression of Multilayer Neural Network,” *IEEE Transactions on Neural Networks and Learning Systems*, vol. 30, no. 5, pp. 1497–1511, May 2019. [Online]. Available: <https://ieeexplore.ieee.org/document/8480873/>
- [60] U. Alon, *An Introduction to Systems Biology: Design Principles of Biological Circuits*. Hoboken: CRC Press, 2006, oCLC: 908078755. [Online]. Available: <http://www.crcnetbase.com/isbn/9781420011432>
- [61] R. Q. Quiroga, L. Reddy, G. Kreiman, C. Koch, and I. Fried, “Invariant visual representation by single neurons in the human brain,” *Nature*, vol. 435, no. 7045, pp. 1102–1107, Jun. 2005. [Online]. Available: <http://www.nature.com/articles/nature03687>
- [62] A. Gonzalez-Garcia, D. Modolo, and V. Ferrari, “Do semantic parts emerge in Convolutional Neural Networks?” *arXiv:1607.03738 [cs]*, Sep. 2017, arXiv: 1607.03738. [Online]. Available: <http://arxiv.org/abs/1607.03738>
- [63] D. Erhan, Y. Bengio, A. Courville, and P. Vincent, “Visualizing higher-layer features of a deep network,” *Technical Report, Univerist de Montral*, 01 2009.
- [64] K. Simonyan, A. Vedaldi, and A. Zisserman, “Deep Inside Convolutional Networks: Visualising Image Classification Models and Saliency Maps,” *arXiv:1312.6034 [cs]*, Apr. 2014, arXiv: 1312.6034. [Online]. Available: <http://arxiv.org/abs/1312.6034>
- [65] A. Mordvintsev and M. Olah, Christopher Tyka, “Inceptionism: Going Deeper into Neural Networks,” 2015. [Online]. Available: <http://ai.googleblog.com/2015/06/inceptionism-going-deeper-into-neural.html>
- [66] A. Nguyen, A. Dosovitskiy, J. Yosinski, T. Brox, and J. Clune, “Synthesizing the preferred inputs for neurons in neural networks via deep generator networks,” *arXiv:1605.09304 [cs]*, Nov. 2016, arXiv: 1605.09304. [Online]. Available: <http://arxiv.org/abs/1605.09304>
- [67] A. Nguyen, J. Clune, Y. Bengio, A. Dosovitskiy, and J. Yosinski, “Plug & Play Generative Networks: Conditional Iterative Generation of Images in Latent Space,” *arXiv:1612.00005 [cs]*, Apr. 2017, arXiv: 1612.00005. [Online]. Available: <http://arxiv.org/abs/1612.00005>
- [68] C. Olah, A. Mordvintsev, and L. Schubert, “Feature visualization,” *Distill*, 2017, <https://distill.pub/2017/feature-visualization>.
- [69] F. Hohman, H. Park, C. Robinson, and D. H. Chau, “Summit: Scaling Deep Learning Interpretability by Visualizing Activation and Attribution Summarizations,” *arXiv:1904.02323 [cs]*, Sep. 2019, arXiv: 1904.02323. [Online]. Available: <http://arxiv.org/abs/1904.02323>
- [70] S. Carter, Z. Armstrong, L. Schubert, I. Johnson, and C. Olah, “Activation atlas,” *Distill*, 2019, <https://distill.pub/2019/activation-atlas>.